

Critical properties of loop percolation models with optimization constraints

Frank O. Pfeiffer and Heiko Rieger

Theoretische Physik, Universität des Saarlandes, 66041 Saarbrücken, Germany

(Dated: June 24, 2018)

We study loop percolation models in two and in three space dimensions, in which configurations of occupied bonds are forced to form closed loop. We show that the uncorrelated occupation of elementary plaquettes of the square and the simple cubic lattice by elementary loops leads to a percolation transition that is in the same universality class as the conventional bond percolation. In contrast to this an optimization constraint for the loop configurations, which then have to minimize a particular generic energy function, leads to a percolation transition that constitutes a new universality class, for which we report the critical exponents. Implication for the physics of solid-on-solid and vortex glass models are discussed.

PACS numbers: 64.60.Ak, 64.60.Cn, 64.60.Fr

I. INTRODUCTION

The percolation of loops (or closed strings) appears naturally in the context of liquid helium [1, 2], early universe [3, 4] and high-temperature superconductors [5, 15], where loops represent world-lines, cosmic strings and vortex loops, respectively. In analogy to the characteristic size of a cluster in conventional site or bond percolation [6], the typical diameter ξ of the loops diverges when approaching a critical point, the loop percolation transition. This transition shows power-law behavior at the critical point, which is described by a set of critical exponents that constitute a universality class.

In this paper we study these percolation transitions numerically. We show that the loop percolation (LP) model, in which each elementary plaquette of a square lattice (in $2d$) or on a simple cubic lattice (in $3d$) is occupied with a probability p with an elementary loop, is in the same universality as the conventional d -dimensional bond percolation. More importantly we also show that in contrast to the LP model an optimization constraint for the loop configurations, which then have to minimize a particular generic energy function, leads to a percolation transition that constitutes a new universality class, for which we report the critical exponents.

These *loop Hamiltonian* (LH) models are relevant for the ground state properties of disordered solid-on-solid models [11, 12, 13] and vortex glasses [14]. One particular example of was recently studied by us in the context of a $3d$ vortex glass model for amorphous high- T_c superconductors in the strong screening limit [15], which shows an unconventional percolation transition of vortex loops in the ground state as a function of the disorder strength σ .

The paper is organized as follows: In section II, we introduce the models and the definition of *loops* (clusters). In section III we locate the percolation transition in each model and calculate the critical exponents using finite-size scaling (FSS). Section IV concludes the paper with a summary and a discussion.

II. MODELS

Consider a d -dimensional hyper-cubic lattice - i.e. a square lattice in $2d$ or a simple cubic lattice in $3d$ - of linear size L ($L = 7$ in the $2d$ example in Fig.1) with free boundary conditions (f.b.c.). In the loop percolation (LP) model the elementary plaquettes of the lattice are occupied with elementary loops with a probability p_1 . (There are $(L - 1)^2$ elementary plaquettes in $2d$ and $3L(L - 1)^2$ elementary plaquettes in $3d$.) An elementary loop consists of the four bonds belonging to an elementary plaquette plus a randomly chosen direction: either clockwise or counterclockwise both with probability $1/2$ (see Fig. 1). When two adjacent plaquettes are occupied by elementary loops of same orientation we cancel the occupation of the common bond as indicated in Fig. 1.

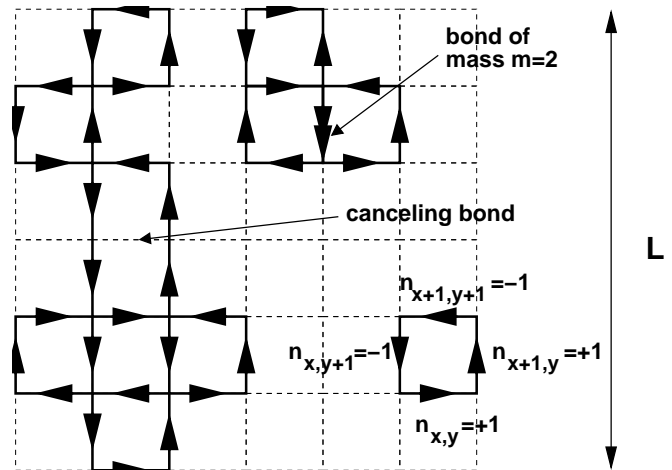


FIG. 1: Configuration \mathbf{n} of the loop percolation model on a $2d$ square lattice with system size $L = 7$.

We can identify the resulting (directed) bond configuration of the LP model with a flow $\mathbf{n} = \{n_1, n_2, \dots, n_M\}$, where n_i is an integer and M is the number of bonds in the lattice. We say that $n_i = 0$ if bond i is not occupied, $n_i = \pm 1$ if it is singly occupied in the positive

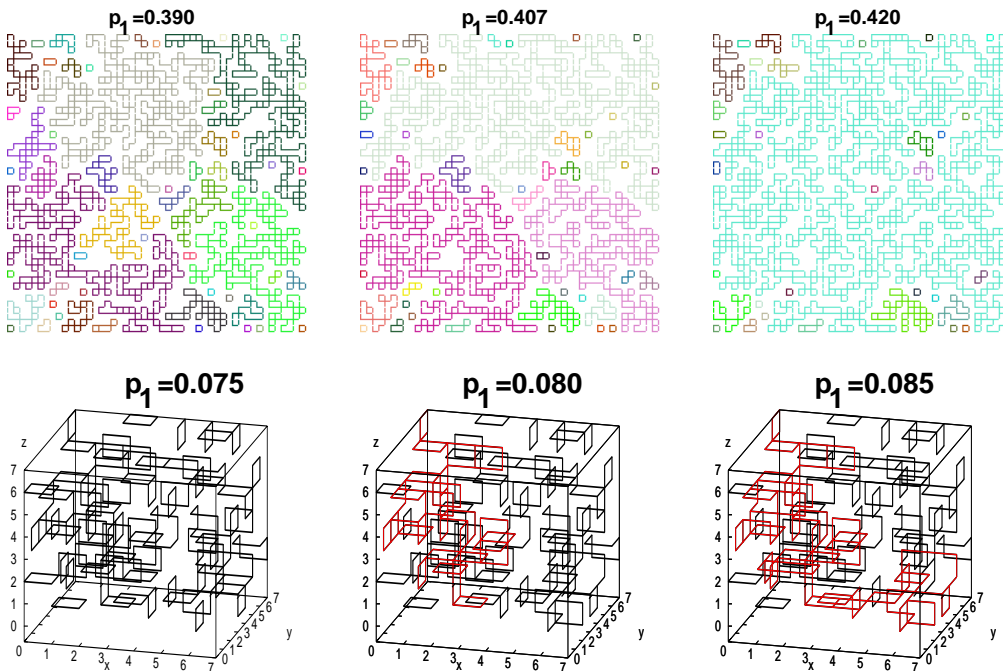


FIG. 2: Typical loop configurations of the LP model around the critical point $p_{1c} \approx 0.41$ in $2d$ (top) for $L = 50$ and $p_{1c} \approx 0.08$ in $3d$ (bottom) for $L = 8$. In $2d$ the different loops are marked by different grey scales (colors), whereas in $3d$ all loops are black except for the percolating loop, which is marked by light grey (red).

(negative) direction (positive and negative are defined by the introduction of an appropriate coordinate system), $n_i = \pm 2$ if it is doubly occupied etc. Thus, an elementary loop (e.g. in the xy plane) can be represented by $n_{x,y} = n_{x+1,y} = -n_{x+1,y+1} = -n_{x,y+1} = 1$ if oriented counterclockwise, as shown in Fig. 1. The complete flow \mathbf{n} then can simply be thought of as the sum of all elementary loops. Obviously, in this sum the flow variables on the common bonds of adjacent elementary loops cancel arithmetically. Moreover, the construction of this flow via addition of elementary loops implies that on each site of the lattice the number of ingoing arrows balances the number of outgoing arrows (see Fig. 1): one says that this flow is divergence free

$$\nabla \cdot \mathbf{n}_i = 0. \quad (1)$$

(The lattice-divergence operator is defined on each lattice site and sums simply all $2 \cdot d$ flow variables of the bonds connected to it).

In analogy to conventional bond percolation we are now going to define the clusters of a configuration of the LP model: Two occupied bonds belong to the same cluster if they have one site in common. Thus, all bonds of the cluster can be connected via a directed path along occupied bonds belonging to this cluster, which is analogous to conventional bond percolation - up to the attribute *directed*. This is actually a slightly non-trivial observation - see Fig. 1 to exemplify this statement - because an occupied directed bond cannot be traversed in the opposite

direction, but is a direct consequence of the fact that a cluster is also a sum of elementary loops.

The mass m of a cluster is the number of occupied bonds, where a bond i with a flow n_i counts $|n_i|$ times, i.e. has mass $m_i = |n_i|$. A percolating cluster is a cluster spanning the entire system (in at least one of the d directions). This implies that the cluster contains a directed path along its occupied bonds from one side of the lattice to the opposite. In the following we refer to the cluster just defined as a loop.

The representation of the configuration of directed occupied bonds as a flow \mathbf{n} is now used to define the LP model *with* an optimization constraint: In contrast to the stochastic *uncorrelated* occupation of elementary loops in the LP model above, we now consider a different type of occupation of loops, which results from the minimization of an energy function for a loop configuration \mathbf{n}

$$H = H\{\mathbf{n}\} = \sum_{i=1}^M f_i(n_i), \quad (2)$$

where the sum is over all bonds i on a d -dimensional hyper-cubic L^d lattice with periodic boundary conditions (p.b.c). Herewith we assume the energy function to be composed of solely of local terms $f_i(n)$ with $f_i(n) \geq 0$ and convex (i.e. $f''(n) \geq 0$) for all bonds i and flow (or occupation) values n . Such energy functions are relevant in the context of disordered solid-on-solid models (in $2d$) [11, 12, 13] and vortex glasses (in $3d$) [14] since they

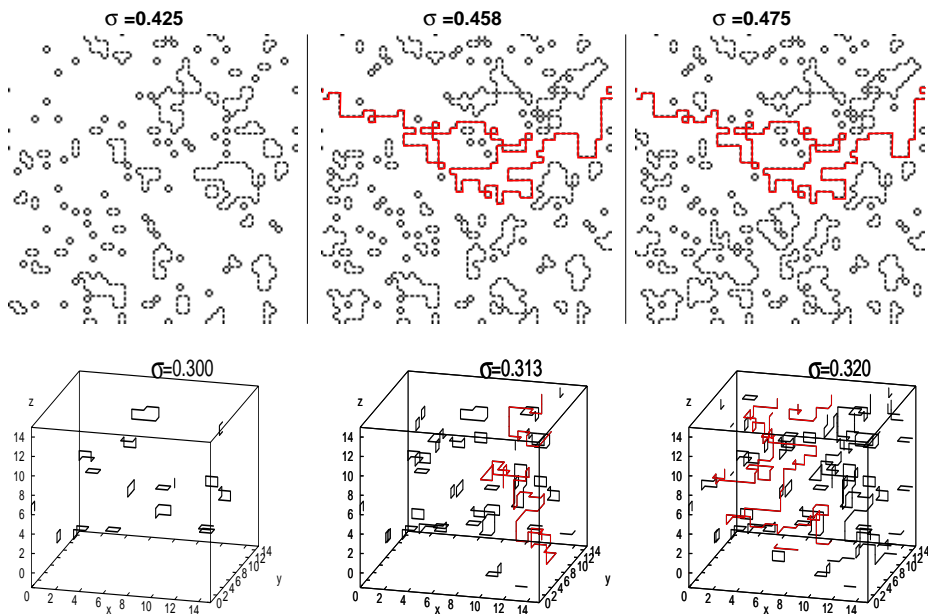


FIG. 3: Typical loop configurations of the loop Hamiltonian (LH) model in the ground state ($T = 0$) around the critical point $\sigma_c \approx 0.46$ in $2d$ (top) for $L = 50$ and $\sigma_c \approx 0.31$ in $3d$ (bottom) for $L = 16$. In $2d$ and $3d$ all loops are black except for the percolating loop, which is marked by light grey (red).

determine their ground states. One has to keep in mind, that the loop condition (1) has to be fulfilled — i.e. the optimization task consist in finding the minimum of (2) under the constraint (1)!

For $f_i(n) = f(n)$ independent of the bond index the minimum is trivial: $n = 0$, i.e. no bond is occupied. Only if the minima of local cost functions vary from bond index to bond index in a non-trivial way one can expect a non-trivial loop configuration. We assume a random distribution of these minima (at values b_i) and restrict ourselves to a quadratic form of $f_i(n)$ around these minima: $f_i(n_i) = (n_i - b_i)^2$, which means that we study the loop configurations (i.e. occupied bond configurations that fulfill (1)) that minimize

$$H = \sum_i (n_i - b_i)^2. \quad (3)$$

The random variables b_i are uniformly distributed $b_i \in [-2\sigma, 2\sigma]$ at a fixed *disorder strength* $\sigma \in [0, 1]$. Here, the probability p to occupy a bond depends on the disorder strength σ . We refer to the LP model *with* an optimization constraint of Hamiltonian (3) as the *loop Hamiltonian* model. For the minimization of a free energy (optimization) we restrict to the calculation of the ground state ($T = 0$) configuration \mathbf{n} , which is a minimum cost flow problem that can be solved *exactly* in polynomial time with appropriate algorithms[7].

III. RESULTS

We use a *depth-first search* algorithm known from combinatorial optimization [7] to identify the connected loops. The number of realizations we used to get statistically averaged data varied from 500 for the largest system size to 20000 for the smallest system size. In the following the error bars of our data in the figures are smaller than the symbol size and are therefore omitted.

Fig. 2 and 3 depict three typical loop configurations of the LP and LH model around the critical threshold, respectively, which clearly indicates a percolation phase transition for both models.

A. Loop percolation model (LP)

First, we study the LP model and consider the probability P^{perc} that a loop percolates the system. Since we assume to have only one typical length scale, which diverges at the critical point like $\xi \sim |p_1 - p_{1c}|^{-\nu}$, in a finite system P^{perc} is expected to scale like

$$P^{perc}(L) \sim \bar{P}[(p_1 - p_{1c}) L^{1/\nu}]. \quad (4)$$

Thus, $P^{perc}(L)$ is independent of L at p_{1c} and the data curves should intersect for different system sizes L . From our raw data in the inset of Fig.4 (left) we locate the critical point $p_{1c} = 0.4070 \pm 0.0005$ in $2d$ and $p_{1c} = 0.0793 \pm 0.0004$ in $3d$, respectively. We plot the scaling assumption (4) in Fig. 4 (left) and estimate the

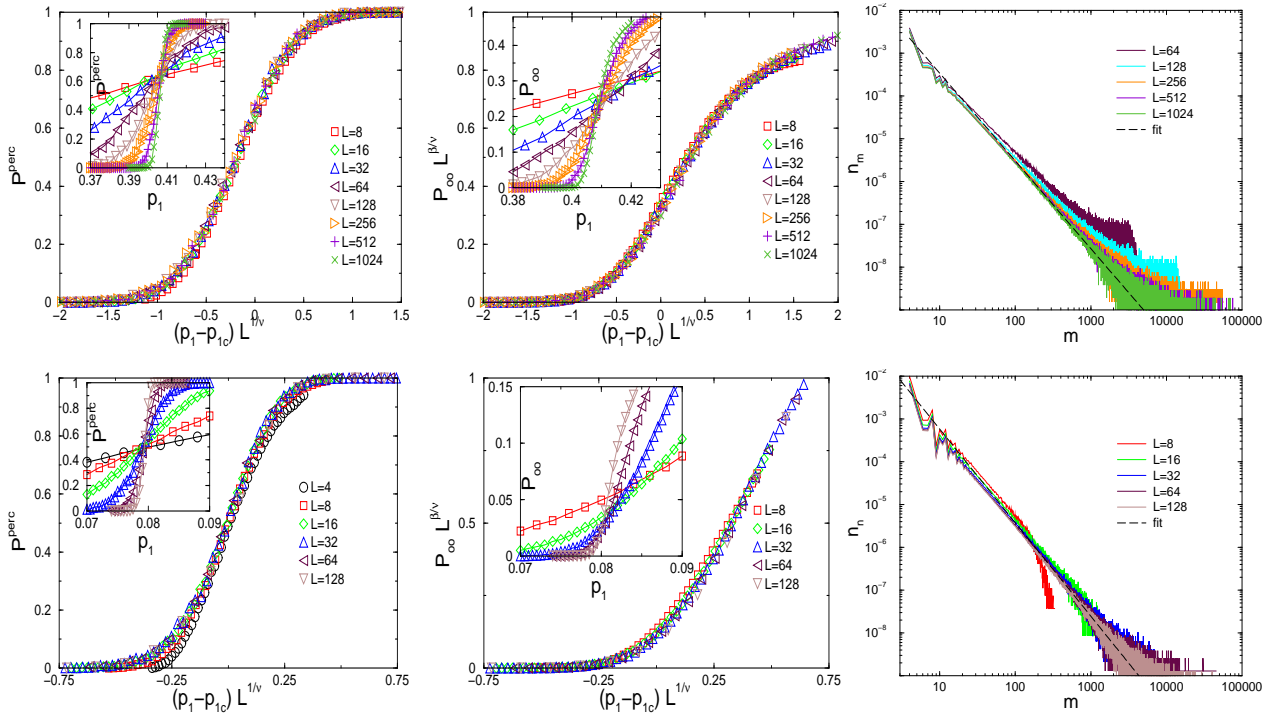


FIG. 4: Finite-size scaling (FSS) for the LP model in $2d$ (top) and $3d$ (bottom): Plot of the percolation probability P^{perc} (left) and of the probability P_∞ for a bond belonging to a percolating loop (middle). The inset shows the raw data. (Right) Plot of the average number n_m of loops of mass m per lattice bond at $p_{1c} = 0.407$ in $2d$ and at $p_{1c} = 0.0793$ in $3d$, respectively.

inverse correlation length exponent $1/\nu = 0.75 \pm 0.03$ in $2d$ and $1/\nu = 1.143 \pm 0.090$ in $3d$ from the best data collapse at fixed p_{1c} .

To get a second critical exponent we consider the probability P_∞ that a bond belongs to the percolating loop, i.e. the order parameter, which is expected to obey

$$P_\infty(L) \sim L^{-\beta/\nu} \bar{P}[(p_1 - p_{1c}) L^{1/\nu}]. \quad (5)$$

Fig. 4 (middle) shows the raw data (inset) and the plot of the scaling law (5) with $\beta/\nu = 0.104 \pm 0.020$ in $2d$ and $\beta/\nu = 0.49 \pm 0.02$ in $3d$ such as to achieve the best data collapse. From the ν above we determine β shown in Table I.

At the critical point p_{c1} the average number n_m of finite loops of mass m per lattice bond scales like

$$n_m(L, p_1 = p_{1c}) \sim m^{-\tau}, \quad (6)$$

where τ is the Fisher exponent [6, 8]. Since we assume the usual scaling relations of conventional percolation to be valid [6], we also expect a combination of them to be valid, i.e. the hyperscaling relation

$$\tau = \frac{2 - \beta/(d\nu)}{1 - \beta/(d\nu)}, \quad (7)$$

where d is the spatial dimension. From the fit of the data of $n_m(L)$ at p_{c1} in Fig. 4 (right) we get τ depicted in Table I. This is consistent with the value from putting

the above ν and β into Eq. (7), i.e. $\tau = 2.05 \pm 0.05$ in $2d$ and $\tau = 2.20 \pm 0.06$ in $3d$.

To determine the critical probability p_c that a bond is occupied we calculate

$$p_c(L) = \sum_{m=4}^{m_L} m n_m(L; p_1 = p_{1c}), \quad (8)$$

where m_L is the largest finite loop. We plot $p_c(L)$ versus $1/L$ as depicted in Fig. 6 and extract p_c from the limit $L \rightarrow \infty$.

In addition to the results presented so far, we found that the mean number N^{perc} of percolating loops per sample in the finite system can be described by a smeared step function with an upper boundary $N^{perc} = 1$ as known from conventional percolation [6]. When we define the mass m_i of an occupied bond i to be $m_i = 1$ even for $|n_i| > 1$, the critical scaling behavior remains unchanged and the critical probability becomes $p_c = 0.565 \pm 0.005$ in $2d$ and $p_c = 0.266 \pm 0.005$ in $3d$, respectively. We also studied the case, where the algorithm detects the loops along oriented paths, and found the same results, as expected from what we said above.

B. Loop hamiltonian model (LH)

For the loop Hamiltonian (3) we perform analogous data analysis. From the intersection of the L -dependent

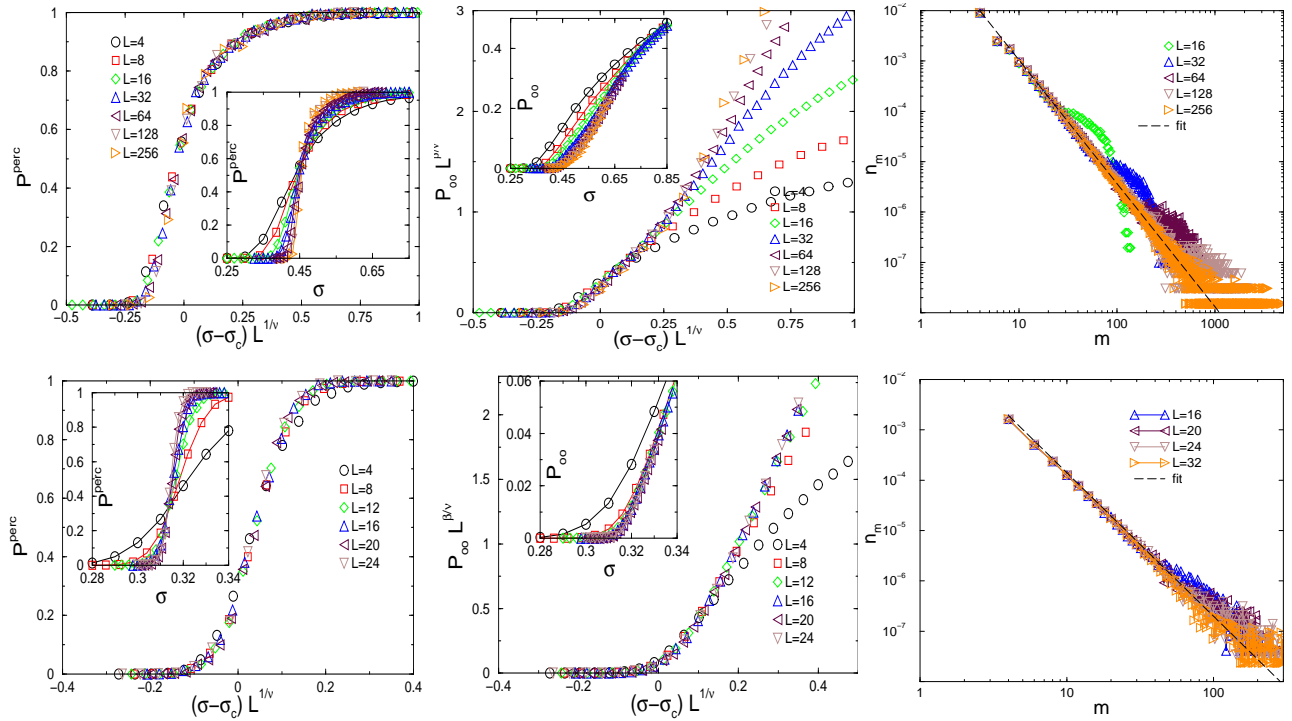


FIG. 5: FSS for the loop Hamiltonian (LH) model in 2d (top) and 3d (bottom). Plot of the percolation probability P^{perc} (left) and of the probability P_∞ for a bond belonging to a percolating loop (middle). The inset shows the raw data. (Right) Plot of the average number n_m of loops of mass m per lattice bond at $\sigma_c = 0.458$ in 2d and at $\sigma_c = 0.3129$ in 3d, respectively.

curves of $P^{perc}(L)$ in the inset of Fig. 5 (left) we locate the critical disorder strength at $\sigma_c = 0.458 \pm 0.001$ in 2d and $\sigma_c = 0.3129 \pm 0.0005$ in 3d, respectively. From the finite-size scaling behavior of the percolation probability P^{perc} (similar to Eq. (4)) we get $1/\nu = 0.30 \pm 0.05$ in 2d and $1/\nu = 0.95 \pm 0.05$ in 3d. The resulting exponent ν are given in Table I. In 2d we find a value $\nu = 3.3 \pm 0.3$, which is rather large.

Fig. 5 (middle) shows the plot of the raw data of P_∞ (inset) and its scaling law similar to Eq. (5) with $\beta/\nu = 0.55 \pm 0.05$ in 2d and $\beta/\nu = 1.30 \pm 0.05$ in 3d. From the ν above we determine β in Table I.

In Fig. 5 (right) we plot the loop distribution $n_m(L)$ vs. the mass m at the critical point σ_c and determine τ by power law fit, which gives the values shown in Table I. From ν and β above we get via the hyperscaling relation (7) the Fisher exponent $\tau = 2.38 \pm 0.17$ in 2d and $\tau = 2.76 \pm 0.26$ in 3d, which are consistent with the values from the power-law fit within the error bars.

In Fig. 7 we plot the mean number N^{perc} of percolating loops per sample. The different curves of $N^{perc}(L)$ intersect at the same critical point σ_c found for P^{perc} above. Similar to the scaling law of $N_{conv.}^{perc}(L)$ in conventional percolation [6] we expect $N^{perc}(L)$ to obey

$$N^{perc}(L) \sim \bar{N}[(\sigma - \sigma_c) L^{1/\nu}], \quad (9)$$

and estimate the same ν as above from the best data collapse, see Fig. 7.

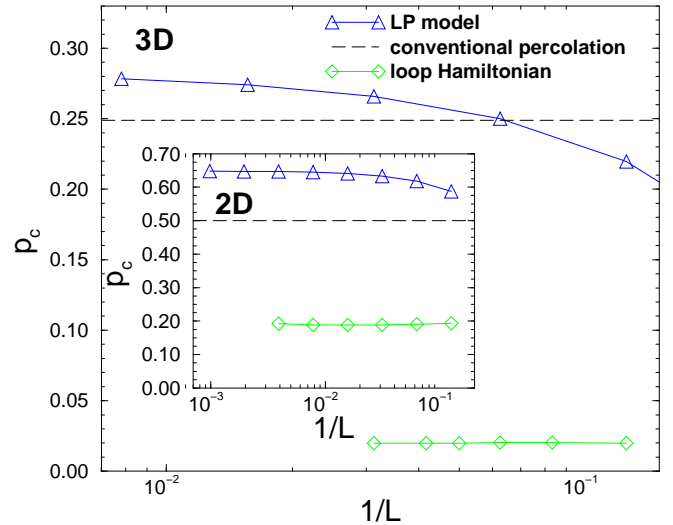


FIG. 6: Plot of the critical probability $p_c(L)$ vs. inverse system size $1/L$ in 2d and in 3d for the conventional percolation model, the LP model and the loop Hamiltonian (LH) model.

The mean number N^{perc} of percolating loops per sample can become larger than one slightly above the critical point σ_c in contrast to conventional percolation, where only one percolating cluster exists for $p > p_c$. The appearance of several percolating loops can possibly be re-

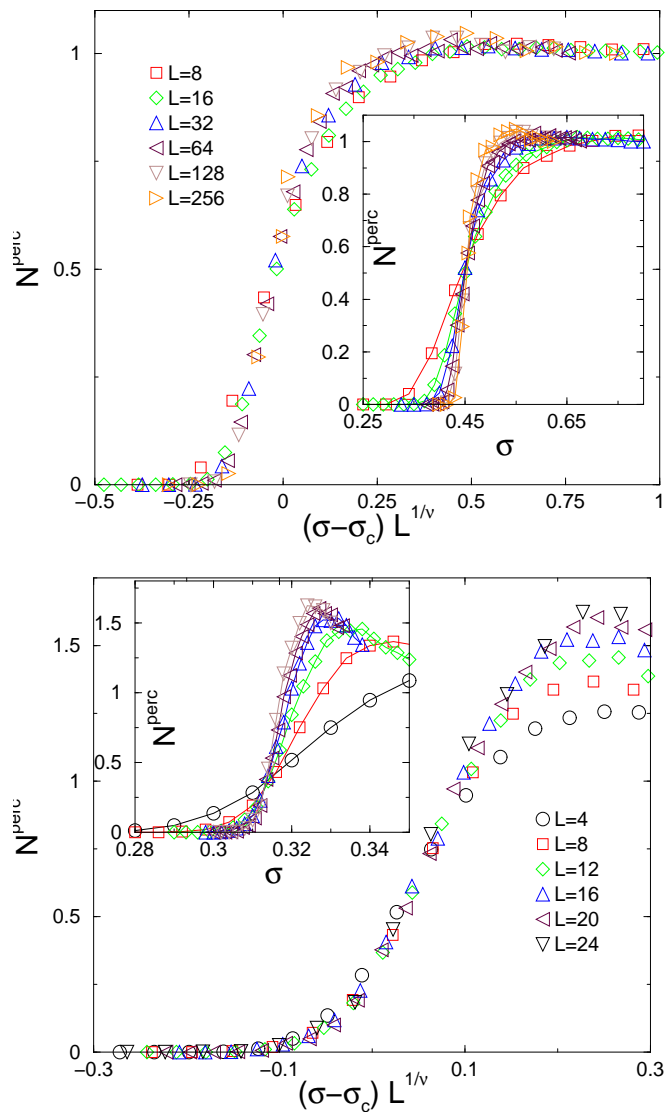


FIG. 7: Plot of the mean number N^{perc} of percolating loops for the loop Hamiltonian (LH) model in $2d$ (top) and $3d$ (bottom).

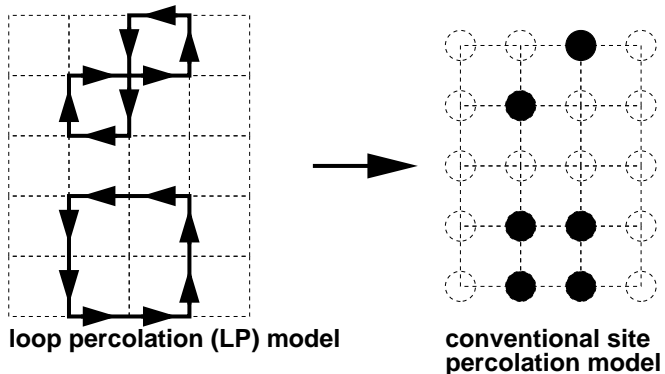


FIG. 8: Schematic mapping of the loops in the LP model (left) onto sites (filled circles) in the conventional site percolation model with next nearest neighbors (right; see text).

lated to the fact that the loop density in the LH model at σ_c is much smaller than in the LP model, as can be seen from comparison of typical loop configurations (c.f. Fig. 2 and 3). Moreover, the maximum of $N^{perc}(L)$ seems to increase with increasing L . From our data we could not determine the behavior of the maximum of $N^{perc}(L)$ in the thermodynamic limit $L \rightarrow \infty$, in particular whether it converges to a constant or diverges. We also checked a L -dependent power law behavior of $N^{perc}(L)$ similar to Eq. (5) with a new critical exponent x (instead of β) and found $x/\nu = 0.01 \pm 0.01$ in $2d$ and $x/\nu = 0.15 \pm 0.02$ in $3d$, i.e. x close to zero.

Finally, we calculate the probability $p_c(L)$ that a bond is occupied (analogous to Eq. 8) for different L at the critical point σ_c as shown in Fig. 6 and extract p_c as the average value, see Table I.

In all considered ground state configurations of the loop Hamiltonian (3) we found a bond to be empty or singly occupied only. Due to this observation we also investigated - beside the study presented this paper - a modified LP model, in which a plaquette is allowed to be occupied with p_1 if and only if the amount of the resulting flow \mathbf{n} is $|n_i| \leq 1$. Here, the algorithm checked each plaquette to be occupied or not in positional order. Note that this occupation process depends on the algorithmic order of occupying plaquettes in the system. Again, we found the same critical exponents as known from conventional percolation, but a different critical probability p_{1c} .

We also studied the $2d$ LH model with a different probability distribution function $P(b_i)$, where b_i is given by a sum of two uniformly distributed random numbers out of $[0, 2\sigma]$. This corresponds to the solid-on-solid (SOS) model on a disordered substrate, which has been studied [11, 12] only at $\sigma = 1/2$ yet. For this probability distribution function we get the same critical exponents as found above, but with a different critical point at $\sigma_c = 0.395 \pm 0.005$, i.e. $p_c = 0.34 \pm 0.02$. This implies that our study is relevant to describe a disorder-driven flat-to-superrough phase transition, not studied in literature yet.

Closely related to the SOS model is the $2d$ model of a random elastic medium with contour loops, for which Zeng et al. found [13] the geometrical exponents $\beta/\nu = d - d_f = 0.54 \pm 0.01$ and $\tau = 2.32 \pm 0.01$ at $\sigma = 1/2$. These exponents agree with the critical $\beta/\nu = 0.55 \pm 0.05$ and $\tau = 2.38 \pm 0.17$ we found here at $\sigma_c \approx 0.458$.

IV. SUMMARY

We studied two loop percolation models, numerically: in the *loop percolation* (LP) model the loop configuration resulted from an uncorrelated unbiased random occupation of elementary directed plaquettes, while in the *loop Hamiltonian* (LH) model the loop configuration appeared according to the Boltzmann weight of a particular microscopic model at $T = 0$, i.e. from an optimization

	conventional percolation [6]	conventional bond percolation [18]	LH	LP	LP with singly occupied bonds
$2d$ p_c	0.5927460^a and $1/2^b$	0.5000 ± 0.0004	0.189 ± 0.005	0.650 ± 0.005	0.570 ± 0.005
p_{1c}				0.4070 ± 0.0005	0.5485 ± 0.0005
σ_c			0.458 ± 0.001		
$P^{perc}(p_c)$		0.70 ± 0.02	0.59 ± 0.02	0.64 ± 0.02	0.67 ± 0.02
ν	$4/3 = 1.\bar{3}$	1.33 ± 0.05	3.33 ± 0.30	1.33 ± 0.05	1.33 ± 0.04
β	$5/36 = 0.13\bar{8}$	0.139 ± 0.030	1.80 ± 0.35	0.138 ± 0.027	0.139 ± 0.007
τ			2.45 ± 0.05	2.05 ± 0.10	
$3d$ p_c	0.31161^a and 0.248814^b	0.2489 ± 0.0002	0.0198 ± 0.0005	0.282 ± 0.005	0.267 ± 0.005
p_{1c}				0.0793 ± 0.0004	0.0992 ± 0.0005
σ_c			0.3129 ± 0.0005		
$P^{perc}(p_c)$		0.63 ± 0.02	0.34 ± 0.02	0.53 ± 0.02	0.54 ± 0.02
ν	0.875	0.875 ± 0.070	1.05 ± 0.05	0.875 ± 0.070	0.875 ± 0.070
β	0.417	0.43 ± 0.04	1.4 ± 0.1	0.43 ± 0.04	0.42 ± 0.04
τ			2.85 ± 0.05	2.19 ± 0.05	

TABLE I: Comparison of the critical thresholds and critical exponents for conventional bond percolation, the loop percolation (LP) model and the loop Hamiltonian (LH) model. ^a refers to conventional site percolation and ^b refers to conventional bond percolation.

constraint (1) of a Hamiltonian (3). Our results are summarized in Table I.

We found that in $2d$ and $3d$ the LP model belongs to the universality class of the conventional (bond or site) percolation [6]. A plausible explanation for this observation is the following: We map an occupied (empty) plaquette onto a occupied (empty) site on an appropriate lattice. Fig. 8 illustrates the mapping in $2d$: the two loops on a square lattice of system size L , Fig. 8 (left), are mapped onto two clusters consisting of 2 and 4 occupied sites on a (dual) square lattice of size $L - 1$, Fig. 8 (right). The resulting clusters of sites are clusters of finite extended objects like k -mers in Ref. [9], which show the same universal behavior at the percolation transition as conventional site percolation [6]. Also we found that the non-trivial orientation of the loops in the LP model is irrelevant for the universality class. We expect that this also holds for higher spatial dimensions d with the same critical dimension $d_c = 6$ as for conventional percolation [6, 10].

For the loop Hamiltonian (LH) model Eq. (3) we found evidence for an unconventional universality class of percolation in $2d$ and $3d$, the exponents are listed in table I. In $2d$, we obtained a rather large correlation length

exponent $\nu = 3.3 \pm 0.3$, which possibly indicates an infinite critical exponent for $L \rightarrow \infty$ known from the Kosterlitz-Touless (KT) phase transition [16]. On the other hand, since our Hamiltonian (3) has no XY, a Kosterlitz-Touless (KT) transition can be ruled out. Indeed, from applying a KT-form of finite-size scaling to our data, we could not find any acceptable data collapse. We like to remark that loop percolation with a large correlation exponent ν also appears in integer Quantum Hall systems, where the loops represent equipotential lines [17].

It would be interesting to study the universal behavior of the pure (i.e. $\sigma = 0$) LH model (3) for finite temperatures T . In $3d$, such a thermal-driven loop percolation phase transition has been studied [5] for a different model.

Acknowledgments

We thank Jae Dong Noh for fruitful discussions and stimulating ideas. This work has been supported financially by the Deutsche Forschungsgemeinschaft (DFG).

-
- [1] Williams G, A Phys. Rev. Lett. **59** 1926 (1989) and literature in there.
 - [2] A. Schakel, Percolation, Bose-Einstein Condensation, and String Proliferation, Phys. Rev. E **63** 026115 (2001).
 - [3] Williams G A, Phys. Rev. Lett. **82** 1201 (1999) and literature in there.
 - [4] Karl Strobl and Mark Hindmarsh, Phys. Rev. E **55** 1120

(1997).

- [5] A. K. Nguyen and A. Sudbø, *Phys. Rev. B* **58** 2802 (1998).
- [6] D. Stauffer, *Introduction to Percolation Theory*, London and Philadelphia, Taylor & Francis (1985); A. Bunde and S. Havlin, *Fractals and Disordered Systems*, 2nd ed., Springer (1996).

- [7] A. Hartmann and H. Rieger, *Optimization Algorithms in Physics*, Wiley-VCH Verlag Berlin (2002).
- [8] M. E. Fisher, *Physics* **3** 255 (1967).
- [9] Y. Leroyer and E. Pommiers, *Phys. Rev. B* **50** 2795 (1994).
- [10] J. Cardy, *Scaling and Renormalization in Statistical Physics*, Cambridge Lecture Notes (1997).
- [11] H. Rieger and U. Blasum, *Phys. Rev. B* **55** 7394 (1997).
- [12] F. O. Pfeiffer and H. Rieger, *J. Phys. A-Math. Gen.* **13** 2489 (2000).
- [13] C. Zeng and J. Kondev and D. McNamara and A. A. Middleton, *Phys. Rev. Lett.* **80** 109 (1998).
- [14] J. Kisker and H. Rieger, *Phys. Rev. B* **58**, R8873 (1998); F. Pfeiffer and H. Rieger, *Phys. Rev. B* **60**, 6304 (1999).
- [15] F. O. Pfeiffer and H. Rieger, *J. Phys. C Condensed Matter* **14** 2361-2369 (2002).
- [16] J. M. Kosterlitz and D. J. Thouless, *J. Phys. C* **6**, 1181 (1973).
- [17] P. Cain and M. E. Raikh and R. A. Roemer and M. Schreiber, *Phys. Rev. B* **64** 235326 (2001).
- [18] We reproduced the results of conventional bond percolation for comparison, where we used parameters (i.e. number of samples and system sizes) similar to the study of the LP model.